Accepted Manuscript

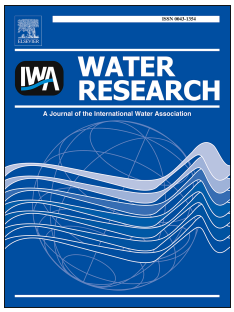

Multiple dynamic Al-based floc layers on ultrafiltration membrane surfaces for humic acid and reservoir water fouling reduction

Baiwen Ma, Wenjiang Li, Ruiping Liu, Gang Liu, Jingqiu Sun, Huijuan Liu, Jiuhui Qu, Walter van der Meer

PII: S0043-1354(18)30296-3

DOI: 10.1016/j.watres.2018.04.012

Reference: WR 13709

To appear in: *Water Research*

Received Date: 14 February 2018

Revised Date: 3 April 2018

Accepted Date: 5 April 2018

Please cite this article as: Ma, B., Li, W., Liu, R., Liu, G., Sun, J., Liu, H., Qu, J., van der Meer, W., Multiple dynamic Al-based floc layers on ultrafiltration membrane surfaces for humic acid and reservoir water fouling reduction, *Water Research* (2018), doi: 10.1016/j.watres.2018.04.012.

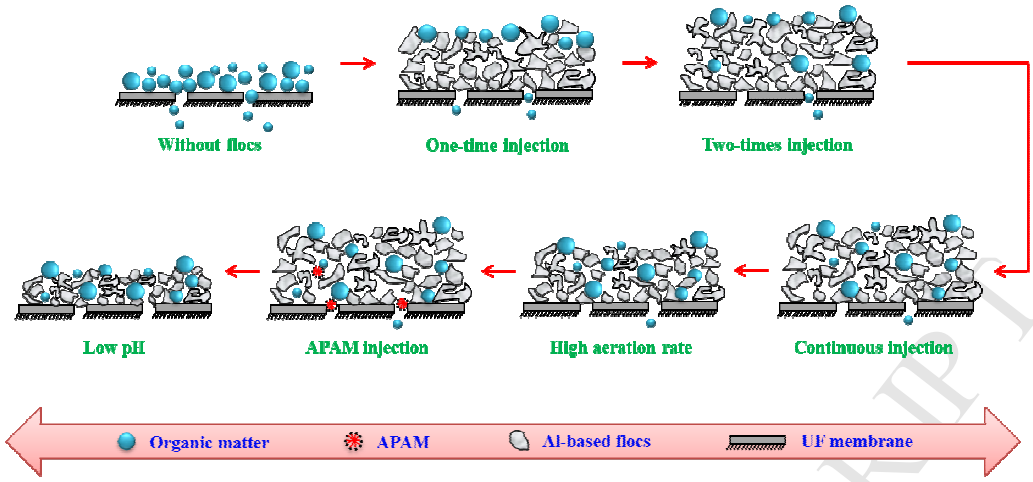

Multiple dynamic Al-based floc layers on ultrafiltration membrane surfaces for humic acid and reservoir water fouling reduction

Baiwen Ma[a], Wenjiang Li[a,b], Ruiping Liu[a,*], Gang Liu[c], Jingqiu Sun[a,d], Huijuan Liu[d,e], Jiuhui Qu[a,d], Walter van der Meer[f]

[a] Key Laboratory of Drinking Water Science and Technology, Research Center for Eco-Environmental Sciences, Chinese Academy of Sciences, Beijing 100085, China

[b] Xi'an University of Architecture and Technology, Shaanxi 710055, China

[c] Sanitary Engineering, Department of Water Management, Faculty of Civil Engineering and Geosciences, Delft University of Technology, P.O. Box 5048, 2600GA Delft, the Netherlands

[d] University of Chinese Academy of Sciences, Beijing 100049, China

[e] State Key Laboratory of Environmental Aquatic Chemistry, Research Center for Eco-Environmental Sciences, Chinese Academy of Sciences, Beijing 100085, China

[f] Science and Technology, University of Twente, P.O. Box 217, 7500AE Enschede, the Netherlands

* Corresponding author. Tel.: +86 10 62849160; Fax: +86 10 62923558;
E-mail address: liuruiping@rcees.ac.cn

Abstract: The integration of adsorbents with ultrafiltration (UF) membranes is a promising method for alleviating membrane fouling and reducing land use. However, adsorbents typically are only injected into the membrane tank once, resulting in a single dynamic protection layer and low removal efficiency over long-term operation. In addition, the granular adsorbents used can cause membrane surface damage. To overcome these disadvantages, we injected inexpensive and loose aluminum (Al)-based flocs directly into a membrane tank with bottom aeration in the presence of humic acid (HA) or raw water taken from the Miyun Reservoir (Beijing, China). Results showed that the flocs were well suspended in the membrane tank, and multiple dynamic floc protection layers were formed (sandwich-like) on the membrane surface with multiple batch injections. Higher frequency floc injections resulted in better floc utilization efficiency and less severe membrane fouling. With continuous injection, acid solutions demonstrated better performance in removing HA molecules, especially those with small molecular weight, and in alleviating membrane fouling compared with the use of high aeration rate or polyacrylamide injection. This was attributed to the small particle size, large specific surface area, and high zeta potential of the flocs. Additionally, excellent UF membrane performance was exhibited by reservoir water with continuous injection and acid solution. Based on the outstanding UF membrane performance, this innovative integrated filtration with loose Al-based flocs has great application potential for water treatment.

Key words: Ultrafiltration membrane; Al-based flocs; Multiple dynamic layers; Humic acid and reservoir water; Fouling reduction.

1 Introduction

Ultrafiltration (UF) membranes, as an advanced separation technology, have been widely used in drinking water and wastewater treatment (Huang et al., 2009; Tang et al., 2017). The installed capacities of low pressure membrane systems have grown exponentially in the last few decades (Furukawa, 2008). However, membrane fouling is inevitable due to the accumulation of pollutants in membrane pores and the formation of dense cake layers. Of most concern, fouling can increase the energy costs of membrane filtration due to the development of large hydraulic resistance and high transmembrane pressure (TMP) (Kimura et al., 2004). As a result, the sustainability of membranes in water treatment is limited.

Most studies have demonstrated that pore constriction, pore blockage and cake layer formation are the main fouling mechanisms of membranes (Huang et al., 2008; Huang et al., 2009; Cai et al., 2013; Polyakov and Zydney, 2013; Tang et al., 2017). Membrane flux can dramatically decrease at the beginning of the filtration process, because many foulant aggregates are deposited on the membrane surface or in membrane pores, leading to pore constriction and blockage. The faster the reduction in membrane flux, the more likely the occurrence of pore constriction and blockage is (Ho and Zydney, 2000). Conversely, when cake layer formation is the main fouling mechanism, membrane flux decline is relatively slow (Wintgens et al., 2003; Wang and Tarabara, 2008; Wu et al., 2011).

To effectively alleviate membrane fouling, different pretreatment technologies, including pre-adsorption, direct filtration, and integrated filtration, have shown

considerable potential in pollutant removal (Kim et al., 2010; Gao et al., 2011; Feng et al., 2015; Yu et al., 2015). Traditional pre-adsorption technology has shown moderately good performance in water treatment plants (Dong et al., 2007; Masmoudi et al., 2016); however, many small molecular weight (MW) substances remain after sedimentation, resulting in severe membrane fouling by pore constriction and dense cake layer formation (Yu et al., 2015). In addition, this technology requires a relatively large land area during actual operation. To overcome these shortcomings, direct filtration, in which the sedimentation tank has been removed, has been researched and applied in water treatment plants (Xiao et al., 2013; Shang et al., 2015; Yu et al., 2015). However, although only a loose cake layer is formed and membrane fouling is alleviated compared with the pre-adsorption process, the sludge production rate is high, resulting in considerable sludge discharge and rapid microbial growth in the membrane tanks (Baker, 2012). To overcome these issues, the emerging technique of integrated filtration has become a new area of focus (Ajmani et al., 2012; Cai et al., 2013; Ma et al., 2015).

In integrated filtration, adsorbents are pre-deposited onto the membrane surface or pre-injected into the membrane tank to form a loose dynamic protection layer, resulting in excellent membrane performance (Kim et al., 2008; Kim et al., 2010; Ajmani et al., 2012; Ma et al., 2013). However, adsorbents are pre-deposited or injected only once, resulting in the formation of a single dynamic layer, with low floc utilization efficiency. As a result, the removal efficiency of pollutants is gradually reduced over time, and a dense cake layer is formed on the protective layer

by pollutants, leading to severe membrane fouling (Ma et al., 2015). In addition, most currently investigated granular adsorbents, including heated iron oxide particles (Zhang et al., 2003), carbon nanotubes (Ajmani et al., 2012), powdered activated carbon (Cai et al., 2013), and nanoscale zerovalent iron (Ma et al., 2015), are either expensive or easily cause membrane surface damage after long-term operation. Thus, for practical operation, it is necessary to explore new adsorbents and methods to further improve the performance of the integrated membrane process.

Aluminum (Al) and iron (Fe) salts are widely used as coagulants and demonstrate high pollutant removal efficiencies. Their excellent performance is due to the stronger adsorption abilities of flocs compared with pre-made adsorbents, especially for organic matter (Kimura et al., 2005; Amjad et al., 2015; Ang et al., 2015; He et al., 2015; Yu et al., 2016). Compared with Fe-based salts, less corrosion occurs in the presence of Al-based salts (Zhao et al., 2011). Herein, to overcome the disadvantages and improve application of integrated filtration in actual operation, inexpensive and loose flocs formed by hydrolysis of Al-based salts were directly injected into a membrane tank in the presence of a hollow fiber UF membrane. To fully utilize the adsorbents and improve membrane performance, the flocs were suspended in the membrane tank by bottom aeration.

Humic substances (HS) commonly exist in natural waters and can range from a few mg/L to a few hundred mg/L C (Wall and Choppin, 2003). However, the presence of HS can cause environmental and health problems, such as providing food for undesirable bacteria in water (Bai and Zhang, 2001). HS can also bind with heavy

metals or biocides, yielding high concentrations of these substances and enhancing their transport in water (Schmitt et al., 2003), and can react with chlorine during water treatment to form disinfection by-products, such as trihalomethane (Wang et al., 2015). Furthermore, HS can compete with low MW synthetic organic chemicals and inorganic pollutants, reducing their adsorption rates and equilibrium capacities (Klausen et al., 2003), and can act as a major foulant, causing serious micro/ultrafiltration membrane fouling due to its large MW distribution (Yuan and Zydeny, 2000).

Herein, to test the integrated floc and UF membrane process, the membrane performance and removal efficiency of HS were investigated. In addition, to fully understand the characteristics of the dynamic protection layer, the factors responsible for membrane fouling, such as injection dosage and frequency, aeration rate, and solution pH, were investigated. Moreover, to clarify the practicability of the integrated floc and UF membrane process, raw water taken from the Miyun Reservoir (N:40^{o}29’; E:116^{o}49’), the main drinking water resource for Beijing, was also investigated.

2 Materials and methods

2.1 Materials

All chemical reagents used, including $AlCl_3 \cdot 6H_2O$, HCl, NaOH, and polyacrylamide, were of analytical grade and were obtained from Sinopharm Chemical Reagent Co., Ltd (China). Deionized (DI, Millipore Milli-Q, USA) water was used in the experiments. Humic acid sodium salt (HA, Sigma-Aldrich, USA), a

HS representative, was dissolved in tap water (Beijing, China) at a concentration of 20 mg/L. All chemical stock solutions were stored in the dark at 4 ^{o}C. Table 1 shows the specific characteristics of the feed water with HA and the specific properties of the source water from Miyun Reservoir.

Table 1

2.2 Floc preparation

For floc preparation, $AlCl_3 \cdot 6H_2O$ was dissolved in 400 mL of tap water (Beijing) each time, with the solution pH adjusted to 7.5 using 1 M NaOH. To prevent high Al concentrations in the effluent after filtration, the prepared flocs were washed with DI water three times before injecting. Almost 60% of Al species are solid hydrolysis products (mainly $Al(OH)_3$) at pH 7.5 (Zhao et al., 2009), with the main characteristics shown in Table S1. Thus, the concentration of the Al-based flocs (calculated as Al, same below) was ~60% of the concentration of the Al-based coagulants.

2.3 Filtration progress

A schematic diagram of the membrane process is shown in Fig. S1. The membrane tank had an inner diameter of 64 mm and a height of 800 mm. A polyvinylidene fluoride (PVDF) hollow fiber membrane (Motimo, China) was used, with a MW cutoff (MWCO) of 100 kDa. The effluent from the submerged membrane module was withdrawn using a peristaltic pump (20 $L \cdot m^{-2} \cdot h^{-1}$). The filtration cycle

was 30 min, followed by 1 min of backwashing (40 $L \cdot m^{-2} \cdot h^{-1}$). A water level gauge was used to control the water level and a ceramic aeration device (diameter: 40 mm) was placed at the bottom to ensure that the flocs were well suspended in the membrane tank. All flocs were prepared just before injection to maintain activity (Chen et al., 2015), and were directly injected into the membrane tank once every 8, 4, or 2 d by syringe or by continuous injection with a peristaltic pump. The TMP was monitored by pressure sensors. The hydraulic retention time was maintained at 2.2 h and the accumulated sludge was not released during filtration. To prevent the formation of biopolymer by the development of microorganisms, the system was operated for 11 d due to residual chlorine (Table 1). Tap water was used to wash away the cake layer on the membrane surface after 8 d of operation. Samples were always taken before the next injection, except under the continuous injection treatment. All experiments were carried out in duplicate.

2.4 Characteristics of flocs in the membrane tank

During filtration, floc samples were taken from below the surface of the suspension in the absence of HA with a hollow glass tube. Floc images were captured using an optical microscope equipped with a CCD camera (GE-5, Aigo, China). The specific surface areas of the flocs were analyzed by the Brunauer-Emmett-Teller method (BET, ASAP2020HD88, USA). The zeta potentials of the flocs before and after adsorption were measured by a nano-particle sizing and zeta potential analyzer (BECKMAN COULTER Ltd., USA).

2.5 Other analytical measurements

The pH was measured by a pH meter (Orion, USA). UF membranes with different MWCO were used to grade HA molecules, and the UF fraction method was used to investigate the corresponding removal efficiencies for different MW distributions (Aiken, 1984; Lin et al., 1999). The MW distributions were determined by gel permeation chromatography (GPC, Agilent Technologies, USA) and removal efficiency was calculated by the difference in peak areas (Ma et al., 2015). Additionally, images of the layered membrane surface were obtained using scanning electron microscopy (SEM, JSM-7401F, JEOL Ltd., Japan).

3 Results

3.1 Effect of floc dosage and injection frequency on TMP development

To determine the membrane performance of the integrated process, TMP development induced by HA with/without flocs was investigated (Fig. 1). Results showed considerable membrane fouling caused by HA alone, and TMP significantly increased to 50.7 kPa on day 8. After careful washing with tap water, the corresponding TMP immediately decreased to 10.1 kPa, indicating that cake layer formation by HA was the main fouling mechanism.

Compared with the TMP caused by HA alone, membrane fouling was alleviated with one-time floc injection, with higher floc doses also resulting in less severe membrane fouling. The TMP values were 33.1, 27.3, and 23.2 kPa in the presence of 6.5, 13.0, and 26.0 mM flocs, respectively, on day 8 (Fig. 1a). After careful washing

208 with tap water, the corresponding TMP dramatically decreased to 6.8, 5.2, and 4.9
209 kPa, respectively.

210 To further clarify membrane performance, TMP development with multiple
211 batch injections was investigated in the presence of 13.0 and 26.0 mM flocs (Figs. 1b
212 and 1c). For 13.0 mM flocs, the TMP was gradually reduced with injections once
213 every 8 (13 mM/time), 4 (6.5 mM/time), and 2 (3.25 mM/time) d, with corresponding
214 TMP values of 27.3, 20.8, and 15.7 kPa, respectively, on day 8. However, the TMP
215 increased to 18.6 kPa by day 8 under continuous injection conditions (0.05 L/h, same
216 below). For 26.0 mM flocs, membrane fouling gradually declined with increasing
217 injection frequency. The corresponding TMP values were 23.2, 18.3, and 15.1 kPa on
218 day 8 following injections once every 8 (26 mM/time), 4 (13 mM/time), and 2 (6.5
219 mM/time) d, respectively. When continuous injections were used, membrane fouling
220 was further alleviated and the TMP was only 10.1 kPa on day 8. As seen from Figs.
221 1b and 1c, the TMP dramatically decreased after careful washing with tap water on
222 day 8, which also showed that cake layer formation was the primary fouling
223 mechanism.

224

225 **Figure 1**

226

227 **3.2 Effect of injection frequency on HA removal efficiency**

228 The UF membrane performed better in the presence of 26.0 mM flocs than 13.0

mM flocs. Thus, 26.0 mM flocs (same below) were further investigated with batch injections (Fig. 2). Figure 2a shows that the concentration of HA in the effluent was reduced with the floc injections. However, the removal efficiency of HA slightly increased after 8 d of operation with one-time injection. The removal efficiency of HA by the membrane alone was 29.2%, but the efficiency only increased to 38.3% in the presence of 26.0 mM flocs on day 8 for the one-time injection mode. Due to the removal of HA molecules, the peak value of HA MW distribution in the effluent declined from 11294.2 Da to 9973.7 Da.

Figure 2b shows that the removal efficiency of HA was gradually reduced over time with one-time injection. The corresponding removal efficiency of HA was 83.1% ± 2.3% on day 2, declining to 38.3% ± 3.1% on day 8. With increasing injection frequency, the removal efficiency of HA increased over time, especially by day 8. The removal efficiency of HA was 38.3 ± 3.1% with one-time injection, but this increased to 69.2 ± 2.2% on day 8 under continuous injection. In addition, the variation in the removal efficiency of HA molecules became smaller with increasing injection frequency. The variation reached 44.8 ± 3.1% between day 2 and day 8 with one-time injection, but decreased to 4.1 ± 1.9% between day 2 and day 8 under continuous injection. Furthermore, the total removal efficiency of HA increased with increasing injection frequency, from 62.2% ± 2.3% with one-time injection to 70.3% ± 2.8% with continuous injection (Fig. S2). Due to the high removal efficiency of HA molecules, the peak value of the HA MW distribution significantly decreased from 9973.7 Da under one-time injection treatment to 7819.1 Da under continuous

injection treatment after 8 d (Fig. 2a).

Due to the large variation in the MW of HA, the corresponding removal efficiencies were further investigated (Fig. 2c). For comparison, the results for permeate samples from a pristine PVDF UF membrane are also presented. As seen from Fig. 2c, the removal efficiency of large HA molecules (>30 kDa) by the membrane alone was 43.1% ± 2.2%, whereas those for the medium (3-30 kDa) and small (<3 kDa) HA molecules were 37.3% ± 1.6% and 6.4% ± 1.8%, respectively, on day 4, with similar results occurring on day 8. When the flocs were injected in batches, the removal efficiencies of the different MW HA molecules were higher on day 8 than on day 4. With increasing injection frequency, the removal efficiency of HA also increased, especially for the smaller molecules. On day 4 and day 8, the removal efficiencies of the small MW HA molecules (<3 kDa) were 19.7% ± 2.6% and 22.9% ± 1.6%, respectively, with injections every 4 d, but increased to 52.9% ± 4.5% and 54.3% ± 3.2%, respectively, under continuous injection treatment. In comparison with the large (>30 kDa) and medium (3-30 kDa) MW HA molecules, the removal efficiency of the small MW HA molecules (<3 kDa) was much lower, which was largely influenced by injection frequency and running time.

Figure 2

3.3 Effect of aeration rate and polyacrylamide on UF membrane performance

Due to its better UF membrane performance (Sections 3.1 and 3.2), continuous injection was further investigated. As aeration rate plays an important role in floc characteristics, including particle size and membrane attachment ability (Ma et al., 2017), UF membrane performance was tested with different aeration rates (Fig. 3). Results showed that TMP development slowed with increasing aeration rate, and was 10.1, 8.8, and 5.8 kPa under 0.1, 0.3, and 0.5 L/min, respectively (Fig. 3a). However, the removal efficiency and peak value variation were influenced little under different aeration rates (Fig. 3b), as reported previously (Ma et al., 2017).

In comparison to the aeration rate, polyacrylamide has the potential to enhance the adsorption ability of flocs (Aguilar et al., 2005). To strengthen the removal efficiency of the multiple layers and reduce membrane fouling, anionic polyacrylamide (APAM) was used due to the positively charged Al-based flocs (1.4 ± 0.3 mV) and negatively charged UF membrane at pH 7.5 (Childress and Elimelech, 1996). However, severe UF membrane fouling occurred as a function of time (Fig. 3c). TMP significantly increased with increasing APAM dosage, from 10.1 kPa to 35.7 kPa (0.1 mg/L) and 76.3 kPa (1 mg/L) on day 8. Figure 3d shows that the removal efficiency of HA was also influenced little in the presence of APAM. The removal efficiency of HA only increased from 70.8% (without APAM) to 76.5% (1 mg/L APAM), and the peak value of HA declined from 7819.1 Da (without APAM) to 7565.8 Da (1 mg/L APAM). In addition, owing to the limited influence of the aeration rate and APAM injection on HA removal, the corresponding removal efficiencies of

different MW HA were similar to those with continuous injection (data not shown).

Figure 3

3.4 Effect of pH on TMP development and HA removal efficiency

Due to the variation in particle size and fractal dimension, solution pH also plays an important role in determining floc characteristics (Feng et al., 2015). Figure 4 shows the UF membrane performance under different pH conditions. As seen from Fig. 4a, the TMP increased much more slowly at pH 6 than at pH 9 over time. After 8 d of operation, the TMP increased to 7.1, 10.1, and 16.3 kPa at pH 6, pH 7.5, and pH 9, respectively. After washing with tap water, the TMP dramatically decreased, indicating that cake layer formation was the primary fouling mechanism.

The corresponding removal efficiencies of HA were 92.9%, 70.8%, and 59.7% at pH 6, pH 7.5, and pH 9, respectively. Along with the removal efficiency of HA, the peak value of HA in the effluent varied, ranging from 11294.2 Da to 5660.5 Da (Fig. 4b). In comparison to the use of high aeration rate and APAM injection, the removal efficiency of different MW HA molecules significantly increased with lower solution pH, especially at pH 6. This showed that large (>30 kDa) and medium (3-30 kDa) MW HA molecules were almost totally removed, and the removal efficiency of small (<3 kDa) MW HA molecules was higher than 90%.

Figure 4

3.5 UF membrane performance with raw water

To test the practicability of the integrated UF membrane process, raw water taken from Miyun Reservoir was used (Table 1). Based on the excellent UF membrane performance presented in Section 3.4, Al-based flocs were also continuously injected into the membrane tank at a pH of 6 and aeration rate of 0.1 L/min. As seen from Fig. 5a, severe UF membrane fouling occurred without pretreatment, and the TMP gradually increased to 15.1 kPa on day 8. However, with the continuous injection of flocs, TMP development was dramatically reduced, and only increased to 4.7 kPa by day 8. After washing, the TMP significantly decreased, indicating that cake layer formation was the main fouling mechanism.

Owing to the existence of DOC (Table 1), the corresponding removal efficiency and MW variation were further investigated. As seen from Fig. 5b, two peak values at 10023.1 Da and 5972.4 Da were observed due to the complexity of the raw water. Compared to the MW distribution of HA (<50 kDa, Fig. 2a), the raw water MW distribution was smaller (<20 kDa). As shown in Fig. 5b, both large (>10 kDa) and small MW organic matter (<10 kDa) were largely removed, with rates of 83.5% and 51.4%. With the removal of organic matter, the large peak gradually declined from 10023.1 Da to 8129.1 Da, though the small peak remained the same before and after filtration (5972.4 Da).

Figure 5

4 Discussion

Due to the large MW distribution of HA molecules, cake layer formation was found to be the primary fouling mechanism during UF membrane filtration (Fig. 1a). The specific particle size distribution of HA was measured (Fig. 6a), showing two peak values (at 14.1 nm, volume: 22.2%; at 141.8 nm, volume: 9.1%) due to the characteristics of HA (Ma et al., 2014). The average membrane pore size, provided by the manufacturer, was 25 nm. Thus, because of large HA molecule interference, the chance of pore constriction/blockage was relatively low, and severe membrane fouling was much more likely caused by dense cake layer formation (Yuan and Zydeny, 2000). The TMP significantly increased to 50.7 kPa on day 8, but immediately decreased to 10.1 kPa after the membrane was washed with tap water.

When flocs were injected into the membrane tank only once, most HA molecules were easily adsorbed or rejected by the flocs. The more flocs were injected, the more HA molecules were removed. As shown in Fig. 6b, the average particle size of the Al-based flocs at pH 7.5 was 161.7 ± 18.6 μm (much larger than the membrane pore diameter) and the specific surface area was 251.7 ± 9.1 m^2/g. As a result, membrane fouling caused by the loose flocs alone was negligible after 8 d of operation (data not shown). The zeta potentials also showed that the HA molecules were easily adsorbed by the Al-based flocs. The zeta potential of the Al-based flocs was 1.4 ± 0.3 mV at pH 7.5, whereas the corresponding zeta potential of the HA molecules was -29.2 ± 3.7 mV. Therefore, a loose cake layer was gradually formed by the flocs after adsorbing HA, leading to the alleviation of membrane fouling,

357 especially under large floc doses (Fig. 1a). The TMP was 50.7 kPa on day 8 in the
358 absence of flocs, but decreased to 33.1, 27.3, and 23.2 kPa in the presence of 6.5, 13.0,
359 and 26.0 mM flocs, respectively.

360

361 **Figure 6**

362

363 When flocs were injected in batches, their utilization efficiency increased due to
364 the multiple floc layers formed. The higher the frequency of the floc injections, the
365 greater the number of dynamic layers that were formed. Figure 7 shows the
366 morphology of the cake layer in the membrane tank on day 8 under an injection
367 frequency of 4 and 2 d (26.0 mM flocs). A floc protection layer was formed with a
368 sandwich-like structure. The average thickness of the floc cake layer was 1.77 ± 0.14
369 mm under 4-d injection frequency, whereas the average thickness was reduced to 0.71
370 ± 0.06 mm under 2-d injection frequency. Although the thickness was smaller under
371 higher injection frequency, more layers were formed, leading to higher HA removal
372 efficiency and slower TMP development (Figs. 1 and 2).

373

374 **Figure 7**

375

376 Because of the particle size distribution of the HA molecules, the corresponding
377 removal efficiency of the UF membrane alone was only 29.2%. When the flocs were
378 injected once, although a protection layer was formed on the membrane surface, most

inner flocs could not be used. Thus, the removal efficiency of HA only increased to 38.3% on day 8 in the presence of 26.0 mM flocs. The higher the injection frequency of the flocs, the greater the number of protection layers formed and the higher the utilization efficiency of the flocs. As a result, continuous injection showed much better performance and the variation in HA removal efficiency was much smaller, with higher total removal efficiency (Fig. S2). In addition, the peak value was further reduced from 11294.2 Da to 7819.1 Da under continuous injection after 8 d (Fig. 2a). It should be noted, however, that once the concentration of HA molecules entering the membrane tank exceeded the maximum adsorption ability with continuous injection, fewer HA molecules were removed and more serious membrane fouling occurred (Figs. 1b and 1c).

For the removal of different MW HA molecules, large (>30 kDa) and medium (3-30 kDa) MW HA molecules were relatively easily removed/rejected by the UF membrane alone due to their large particle size. Although different MW HA molecules could be largely removed in the beginning when flocs were directly injected, many flocs in the inner layer could not be used. As a result, the removal efficiency of different MW HA molecules was reduced over time. Increasing the injection frequency of flocs resulted in an increase in the number of floc layers and the floc utilization efficiency. Thus, the removal efficiency of different MW HA molecules on day 8 was higher than that on day 4 (Fig. 2c). Due to rejection by the dynamic floc layer, the removal efficiency of the small MW HA molecules (<3 kDa) by day 8 significantly increased from 22.9% ± 1.6% with an injection once every 4 d

401 to 54.3% ± 3.2% under continuous injection treatment. As a result of the multiple
402 protection layers, the removal efficiency of the small MW HA molecules (<3 kDa)
403 increased, especially under continuous injection.

404 For the aeration rate, a thinner cake layer was gradually induced with higher
405 aeration rates, leading to smaller cake resistance and slower TMP development. When
406 the aeration rate increased from 0.1 L/min to 0.5 L/min, the average floc size
407 decreased from 161.7 ± 18.6 μm to 132.8 ± 11.7 μm. However, the removal
408 efficiency of HA was almost the same, indicating the full utilization efficiency of the
409 flocs. A potential reason for this is the strong electrostatic attraction between Al-based
410 flocs and HA molecules, whereas the zeta potentials of flocs and HA molecules varied
411 little under different aeration rates. The zeta potential of the Al-based flocs was 1.4 ±
412 0.3 mV at pH 7.5, whereas the corresponding zeta potential of the HA molecules was
413 -29.2 ± 3.7 mV. Thus, the removal efficiency of HA was influenced little by the
414 aeration rate. For APAM, although electrostatic repulsion and attraction occurred
415 between APAM and the negatively charged UF membrane surface and positively
416 charged Al-based flocs, respectively, membrane fouling was more severe compared to
417 that without flocs. The potential reason was that APAM easily adhered to the UF
418 membrane surface during filtration, blocking/covering membrane pores to some
419 extent (Fig. S3). As a result, the higher the concentration of APAM, the more severe
420 the membrane fouling was. In addition, the removal efficiency of HA increased little
421 due to the electrostatic repulsion between the negatively charged APAM and HA
422 molecules at pH 7.5.

Solution pH also played an important role in the floc characteristics. Figure 4 shows that the integrated UF membrane process performed excellently at pH 6, which could be ascribed to the following reasons. Firstly, the floc particle size was 118.2 ± 15.6 µm at pH 6, which increased to 161.7 ± 18.6 µm and 191.7 ± 26.1 µm at pH 7.5 and pH 9, respectively. However, smaller floc particle size results in a larger specific surface area. Here, the specific surface area of the Al-based flocs at pH 6 was 278.8 ± 17.6 m^2/g, which decreased to 251.7 ± 9.1 m^2/g and 206.5 ± 11.2 m^2/g at pH 7.5 and pH 9, respectively. Secondly, the zeta potential of the Al-based flocs was 6.8 ± 0.6 mV at pH 6, but 1.4 ± 0.3 mV and -2.9 ± 0.9 mV at pH 7.5 and pH 9, respectively. As a result, a thinner cake layer and higher removal efficiency of HA was induced at pH 6, resulting in less severe membrane fouling and higher HA removal, even of small MW HA molecules.

For raw water, membrane fouling was also gradually induced as a function of time (Fig. 5a). However, due to the lower DOC concentration of raw water compared to that of 20 mg/L HA (Table 1), less severe UF membrane fouling was induced (Fig. 1a and Fig. 5a). When flocs were continuously injected at pH 6 with 0.1 L/min aeration, a loose cake layer was induced and TMP development became extremely slow. Similar to the removal of HA molecules, although large MW organic matter was preferentially removed during filtration, the removal efficiency of small MW organic matter was also high (51.4%, Fig. 5b).

In view of the above observations, the presence of multiple dynamic floc layers played an important role in removing organic matter and alleviating membrane

445 fouling. When flocs were not injected, limited organic matter passed through the
446 membrane pores and subsequently organic matter formed a dense cake layer on the
447 membrane surface, resulting in serious membrane fouling. When flocs were injected,
448 most organic matters were adsorbed or rejected. The larger the injection frequency,
449 the higher the utilization efficiency of the flocs and the higher the removal efficiency
450 of organic matter. Continuous injection showed much better performance when the
451 input organic matter did not exceed the maximum adsorption ability of the flocs.
452 Additionally, solution pH played a much more important role in alleviating membrane
453 fouling under continuous injection than that of aeration rate or polyacrylamide. The
454 specific schematic diagram regarding the alleviation of membrane fouling is
455 illustrated in Fig. 8. Further study will be conducted on the development of
456 microorganisms and *in situ* chemical cleaning with acid with the existence of flocs
457 after long-term operation.
458
459 **Figure 8**
460

461 ## 5 Conclusions

462 The integrated membrane process is a promising method for alleviating
463 membrane fouling and reducing land use. However, several problems exist with the
464 granular adsorbents used and with the formation of a single dynamic protection layer
465 on the membrane surface due to one-time pre-deposition or injection. To overcome

these problems, inexpensive and loose Al-based flocs were injected into a membrane tank with batch injections and continuous bottom aeration to improve membrane performance.

Results showed that the flocs were well dispersed in the membrane tank and largely adsorbed the HA molecules, leading to less severe membrane fouling. In comparison with one-time injection, a sandwich-like floc cake layer was formed on the membrane surface with batch injections, especially under continuous injection. The flocs were not only fully utilized in the membrane tank, but loose cake layers were gradually formed with continuous injection. In addition, the removal efficiency of small MW HA molecules (<3 kDa) steadily increased with increasing injection frequency. In comparison to aeration rate and polyacrylamide, solution pH showed better efficacy at removing small MW HA molecules and alleviating membrane fouling. Moreover, subsequent raw water experiments confirmed the practicability of the integrated UF membrane under continuous injection with acid solution pH. Based on the excellent membrane performance, this innovative integrated filtration method with loose multiple layers shows great application potential for water treatment.

Acknowledgements

This study was supported by the National Key R&D Program of China (2016YFC0400802), National Natural Science Foundation for Young Scientists of China (51608514), and a special fund from the Key Laboratory of Drinking Water Science and Technology, Research Center for Eco-Environmental Sciences, Chinese

Academy of Sciences (Project No. 17Z03KLDWST).

References

Aguilar, M.I., Sáez, J., Lloréns, M., Soler, A., Ortuño, J.F., Meseguer, V., Fuentes, A., 2005. Improvement of coagulation-flocculation process using anionic polyacrylamide as coagulant aid. Chemosphere 58, 47-56.

Aiken, G.R., 1984. Evaluation of ultrafiltration for determining molecular weight of fulvic acid. Environ. Sci. Technol. 18, 978-981.

Ajmani, G.S., Goodwin, D., Marsh, K., Fairbrother, D.H., Schwab, K.J., Jacangelo, J.G., Huang, H.O., 2012. Modification of low pressure membranes with carbon nanotube layers for fouling control. Water Res. 46, 5645-5654.

Amjad, H., Khan, Z., Tarabara, V.V., 2015. Fractal structure and permeability of membrane cake layers: effect of coagulation-flocculation and settling as pretreatment steps. Sep. Purif. Technol. 143, 40-51.

Ang, W.L., Mohammad, A.W., Teow, Y.H., Benamor, A., Hilal, N., 2015. Hybrid chitosan/$FeCl_3$ coagulation-membrane process: performance evaluation and membrane fouling study in removing natural organic matter. Sep. Purif. Technol. 152, 23-31.

Bai, R., Zhang, X., 2001. Polypyrrole-coated granules for humic acid removal. J. Colloid Interface Sci. 243, 52-60.

Baker, R., 2012. Membrane technology and applications. John Wiley & Sons.

Cai, Z.X., Wee, C., Benjamin, M.M., 2013. Fouling mechanism in low-pressure

membrane filtration in the presence of an adsorbent cake layer. J. Membr. Sci. 433, 32-38.

Chen, X.D., Yang, H.W., Liu, W.J., Wang, X.M., Xie, Y.F., 2015. Filterability and structure of the fouling layers of biopolymer coexisting with ferric iron in ultrafiltration membrane. J. Membr. Sci. 495, 81-90.

Childress, A.E., Elimelech, M., 1996. Effect of solution chemistry on the surface charge on the polymeric reverse osmosis and nanofiltration membranes. J. Membr. Sci. 119, 253-268.

Dong, B.Z., Chen, Y., Gao, N.Y., Fan, J.C., 2007. Effect of coagulation pretreatment on the fouling of ultrafiltration membrane. J. Environ. Sci. 19, 278-283.

Feng, L.J., Wang, W.Y., Feng, R.Q., Zhao, S., Dong, H.Y., Sun, S.L., Gao, B.Y., Yue, Q.Y., 2015. Coagulation performance and membrane fouling of different aluminum species during coagulation/ultrafiltration combined process. Chem. Eng. J. 262, 1161-1167.

Furukawa, D., 2008. A global perspective of low pressure membrane. National Water Research Institute. Fountain Valley (CA).

Gao, W., Liang, H., Ma, J., Han, M., Chen, Z.L., Han, Z.S., Li, G.B., 2011. Membrane fouling control in ultrafiltration technology for drinking water production: a review. Desalination 272, 1-8.

He, Z., Liu, R.P., Liu, H.J., Qu, J.H., 2015. Adsorption of Sb(III) and Sb(V) on freshly prepared Ferric Hydroxide (FeOxHy). Environ. Eng. Sci. 32, 95-102.

Ho, C.C., Zydney, A.L., 2000. A combined pore blockage and cake filtration model

for protein fouling during microfiltration. J. Colloid Interface Sci. 232, 389-399.

Huang, H., Schwab, K., Jacangelo, J.G., 2009. Pretreatment of low pressure membranes in water treatment: a review. Environ. Sci. Technol. 43, 3011-3019.

Huang, H., Spinette, R., O'Melia, C.R., 2008. Direct-flow microfiltration of aquasols: I. impacts of particle stabilities and size. J. Membr. Sci. 314, 90-100.

Kim, J., Cai, Z.X., Benjamin, M.M., 2008. Effects of adsorbents on membrane fouling by natural organic matter. J. Membr. Sci. 310, 356-364.

Kim, J., Cai, Z.X., Benjamin, M.M., 2010. NOM fouling mechanisms in a hybrid adsorption/membrane system. J. Membr. Sci. 349, 35-43.

Kimura, K., Hane, Y., Watanabe, Y., 2005. Effect of pre-coagulation on mitigating irreversible fouling during ultrafiltration of surface water. Water Sci. Technol. 51, 93-100.

Kimura, K., Hane, Y., Watanabe, Y., Amy, G., Ohkuma, N., 2004. Irreversible membrane fouling during ultrafiltration of surface water. Water Res. 38, 3431-3441.

Klausen, J., Vikesland, P.J., Kohn, T., Burris, D.R., Ball, W.P., Roberts, A.L., 2003. Longevity of granular iron in groundwater treatment processes: solution composition effects on reduction of organohalides and nitroaromatic compounds. Environ. Sci. Technol. 37, 1208-1218.

Lin, C.F., Huang, Y.J., Hao, O.J., 1999. Ultrafiltration processes for removing humic substances: effect of molecular weight fractions and PAC treatments. Water Res.

552 33, 1252-1264.

553 Ma, B.W., Wang, X., Liu, R.P., William, A.J., Lan, H.C., Liu, H.J., Qu, J.H., 2017.
554 Synergistic process using Fe hydrolytic flocs and ultrafiltration membrane for
555 enhanced antimony(V) removal. J. Membr. Sci. 537, 93-100.

556 Ma, B.W., Yu, W.Z., Liu, H.J., Qu, J.H., 2014. Effect of low dosage of coagulant on
557 the ultrafiltration membrane performance in feedwater treatment. Water Res. 51,
558 277-283.

559 Ma, B.W., Yu, W.Z., Liu, H.J., Yao, J.B., Qu, J.H., 2013. Effect of iron/aluminum
560 hydrolyzed precipitate layer on ultrafiltration membrane. Desalination 330,
561 16-21.

562 Ma, B.W., Yu, W.Z., William, A.J., Liu, H.J., Qu, J.H., 2015. Modification of
563 ultrafiltration membrane with nanoscale zerovalent iron layers for humic acid
564 fouling reduction. Water Res. 71, 140-149.

565 Masmoudi, G., Ellouze, E., Amar, R.B., 2016. Hybrid coagulation/membrane process
566 treatment applied to the treatment of industrial dyeing effluent. Desalin. Water
567 Treat. 57, 6781-6791.

568 Polyakov, Y.S., Zydney, A.L., 2013. Ultrafiltration membrane performances: effect of
569 pore blockage/constriction. J. Membr. Sci. 434, 106-120.

570 Schmitt, D., Saravia, E., Frimel, F.H., Schuessle, W., 2003. NOM-facilitated transport
571 of metal ions in aquifers: importance of complex-dissociation kinetics and
572 colloid formation. Water Res. 37, 3541-3550.

573 Shang, X., Kim, H.C., Huang, J.H., Dempsey, B.A., 2015. Coagulation strategies to

574 decrease fouling and increase critical flux and contaminant removal in
575 microfiltration laundry wastewater. Sep. Purif. Technol. 147, 44-50.
576 Tang, S.Y., Zhang, Z.H., Zhang, X.H., 2017. New insight into the effect of mixed
577 liquor properties changed by pre-ozonation on ceramic UF membrane fouling in
578 wastewater treatment. Chem. Eng. J. 314, 670-680.
579 Wall, N.A., Choppin, G.R., 2003. Humic acids coagulation: influence of divalent
580 cations. Appl. Geochem. 18, 1573-1582.
581 Wang, F., Tarabara, V.V., 2008. Pore blocking mechanisms during early stages of
582 membrane fouling by colloids. J. Colloid Interface Sci. 328, 464-469.
583 Wang, X.M., Mao, Y.Q., Tang, S., Yang, H.W., Xie, Y.F., 2015. Disinfection
584 byproducts in drinking water and regulatory compliance: a critical review. Front.
585 Env. Sci. Eng. 9, 3-15.
586 Wintgens, T., Rosen, J., Melin, T., Brepols, C., Drensla, K., Engelhardt, N., 2003.
587 Modeling of a membrane bioreactor system for municipal wastewater treatment.
588 J. Membr. Sci. 216, 55-65.
589 Wu, J., He, C.D., Jiang, X.Y., Zhang, M., 2011. Modeling of the submerged bioreactor
590 fouling by the combined pore constriction, pore blockage and cake formation
591 mechanisms. Desalination 279, 127-134.
592 Xiao, F., Xiao, P., Zhang, W.J., Wang, D.S., 2013. Identification of key factors
593 affecting the organic fouling on low-pressure ultrafiltration membranes. J.
594 Membr. Sci. 447, 144-152.
595 Yuan, W., Zyndey, A.L., 2000. Humic acid fouling during ultrafiltration. Environ. Sci.

596 Technol. 34, 5043-5050.

597 Yu, W.Z., Graham, N.J.D., Fowler, G.D., 2016. Coagulation and oxidation for
598 controlling ultrafiltration membrane fouling in drinking water treatment:
599 application of ozone at low dose in submerged membrane tank. Water Res. 95,
600 1-10.

601 Yu, W.Z., Qu, J.H., Gregory, J., 2015. Pre-coagulation on the submerged membrane
602 fouling in nano-scale: effect of sedimentation process. Chem. Eng. J. 262,
603 676-682.

604 Zhang, M.M., Li, C., Benjamin, M.M., Chang, Y.J., 2003. Fouling and natural organic
605 matter removal in adsorbent/membrane systems for drinking water treatment.
606 Environ. Sci. Technol. 37, 1663-1669.

607 Zhao, H., Liu, H.J., Hu, C.Z., Qu, J.H., 2009. Effect of aluminum speciation and
608 structure characterization on preferential removal of disinfection byproduct
609 precursors by aluminum hydroxide coagulation. Environ. Sci. Technol. 43,
610 5067-5072.

611 Zhao, X.L., Zhang, Y.J., 2011. Algae-removing and algicidal efficiencies of
612 polydiallyldimethylammonium chloride composite coagulants in enhanced
613 coagulation treatment of algae-containing raw water. Chem. Eng. J. 173,
614 164-170.

Table 1 Characteristics of feed water

Items	With 20 mg/L HA	Miyun Reservoir water
Water temperature (^{o}C)	18.1 ± 2.8	19.6 ± 1.7
pH	7.4 ± 0.2	8.1 ± 0.3
Turbidity (NTU)	11.8 ± 0.4	1.2 ± 0.3
Conductivity (μs/cm)	93.3 ± 5.1	352.7 ± 10.8
Dissolved organic matter (DOC, mg/L)	6.9 ± 0.7	3.4 ± 0.6
UV_{254} (cm^{-1})	0.5 ± 0.04	0.06 ± 0.01
Residual chlorine (mg/L)	0.5 ± 0.1	-

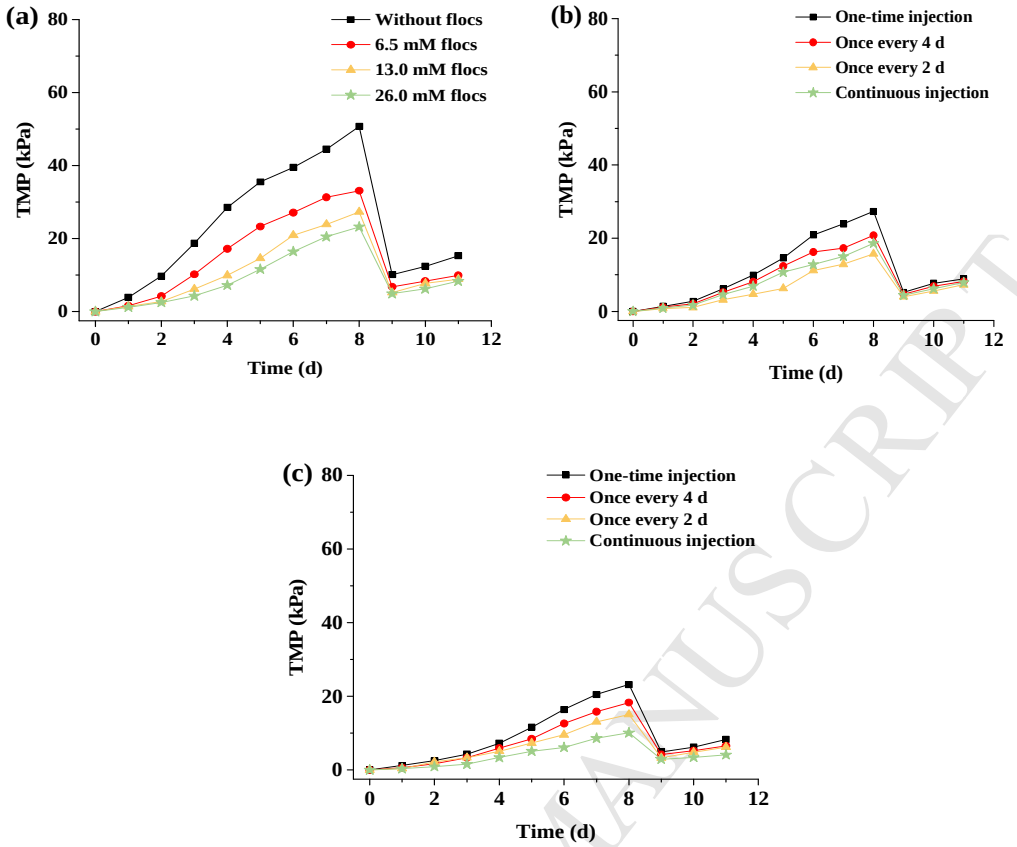

Fig. 1. TMP development over time: (a) Different dosages of flocs with one-time injection; Different injection frequencies in the presence of 13.0 mM flocs (b) and 26.0 mM flocs (c).

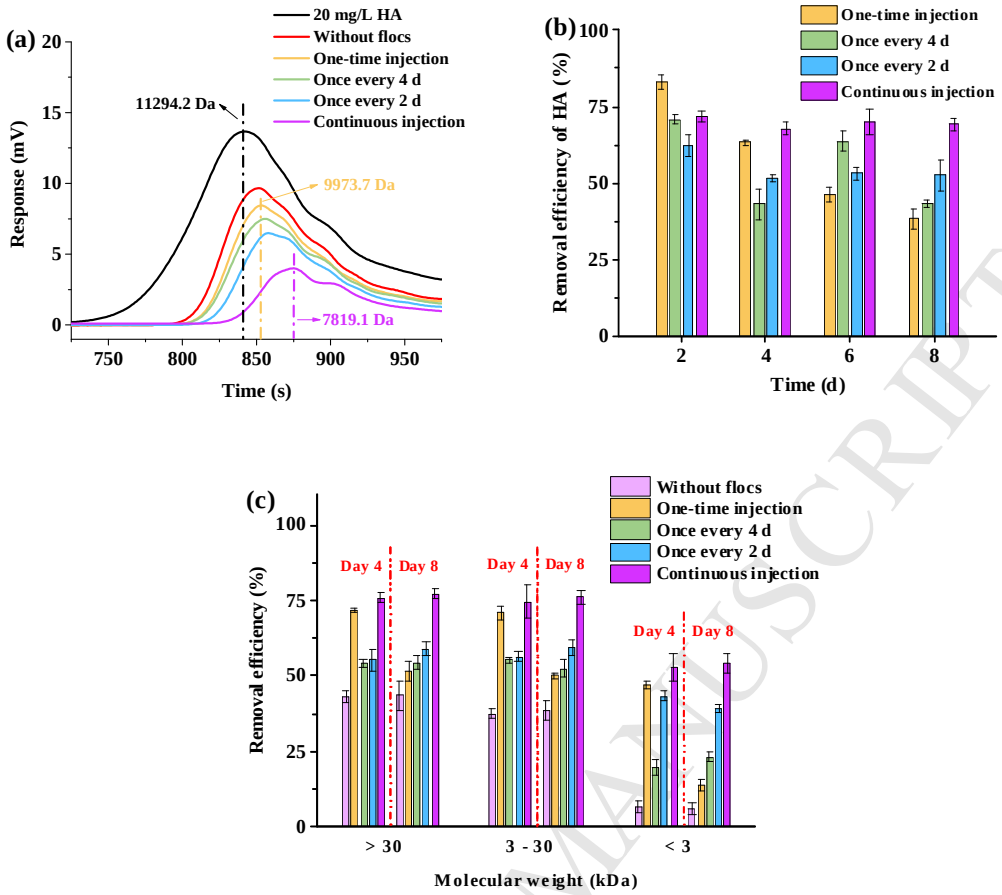

Fig. 2. (a) Concentration and peak value of MW distribution of HA before and after filtration with different injection frequencies on day 8; (b) Removal efficiency of HA with different injection frequencies over time; (c) Removal efficiency of different MW HA molecules with different injection frequencies on day 8.

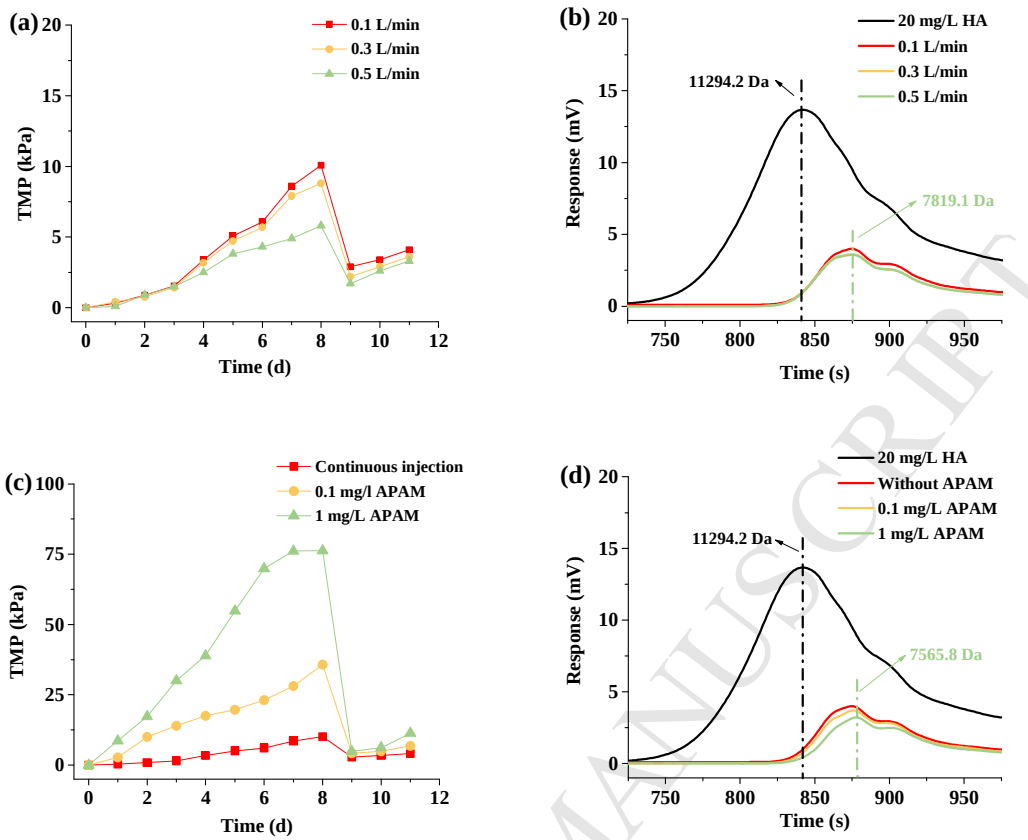

Fig. 3. (a) TMP development with different aeration rates over time; (b) Concentration and peak value of HA MW distribution before and after filtration on day 8; (c) TMP development with different dosages of APAM over time; (d) Concentration and peak value of HA MW distribution before and after filtration with different dosages of APAM on day 8.

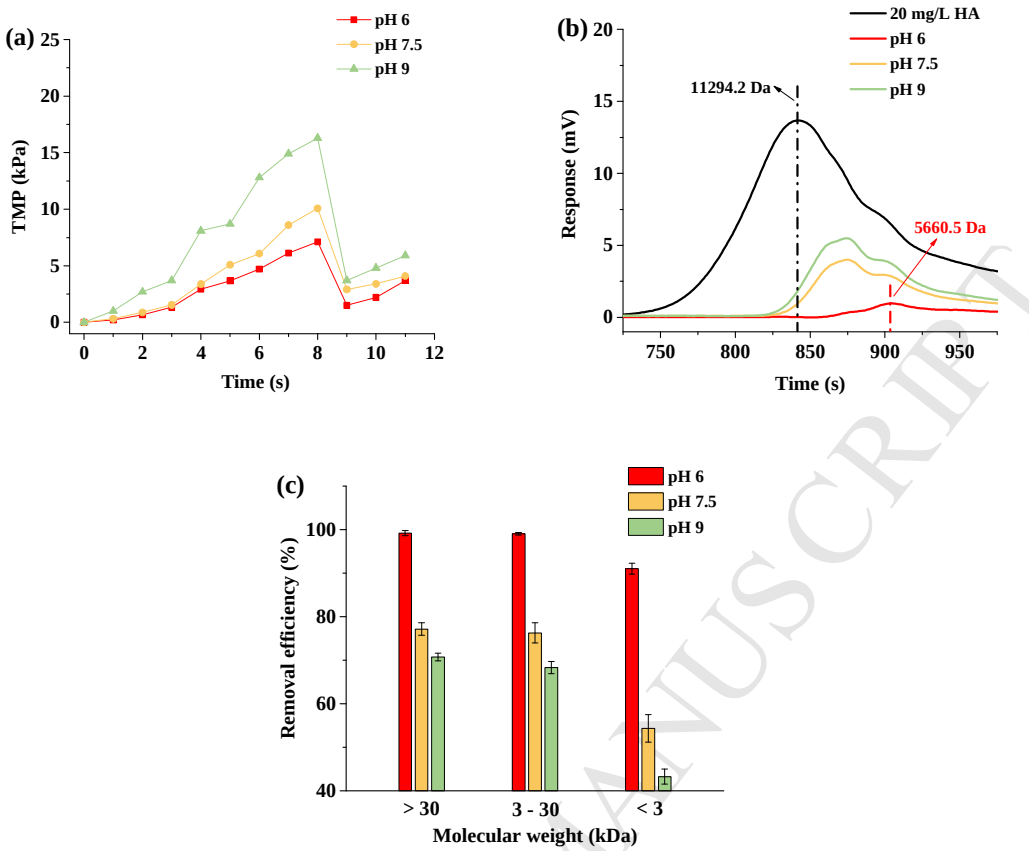

Fig. 4. (a) TMP development under different pH conditions over time; (b) Concentration and peak value of HA MW distribution before and after filtration under different pH conditions on day 8; (c) Removal efficiency of different MW HA molecules under different pH conditions on day 8.

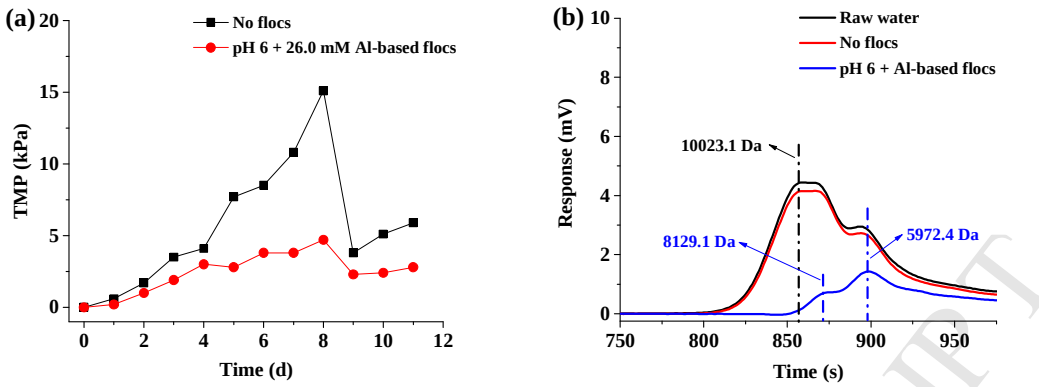

Fig. 5. (a) TMP development as a function of time with raw water; (b) Concentration and peak value of MW distribution of raw water before and after filtration on day 8.

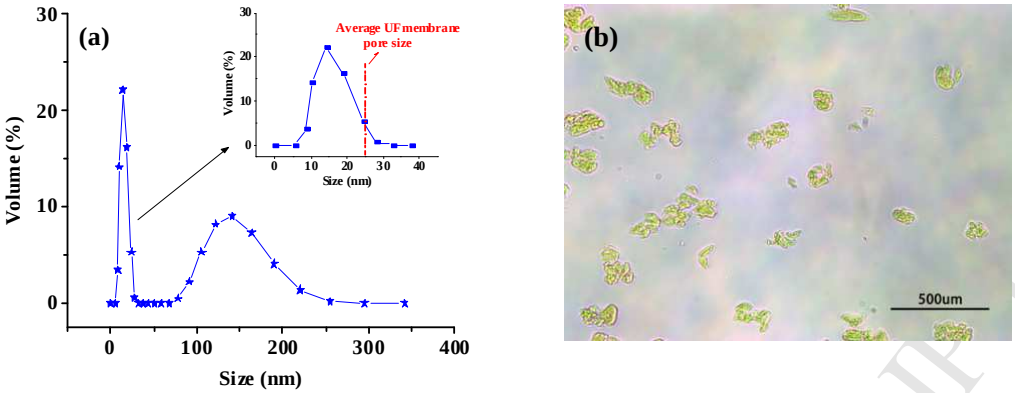

Fig. 6. (a) Particle size distribution of HA molecules in the membrane tank; (b) Images of Al-based flocs in the membrane tank.

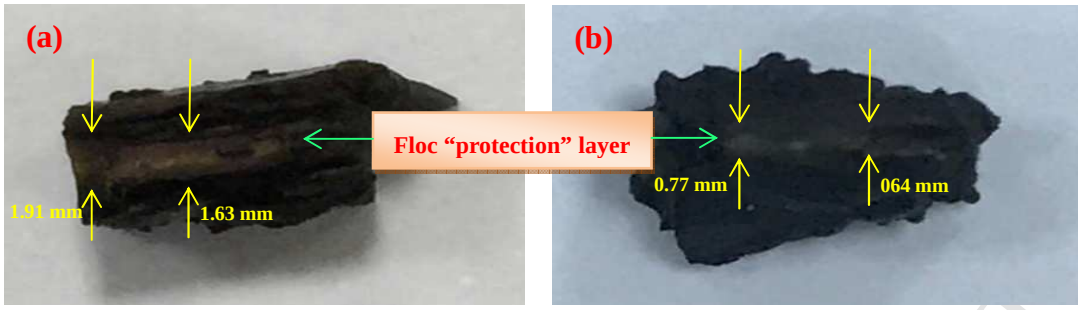

Fig. 7. Morphology of the membrane surface in the tank on day 8 in the presence of 26.0 mM flocs with an injection frequency of (a) 4 d and (b) 2 d.

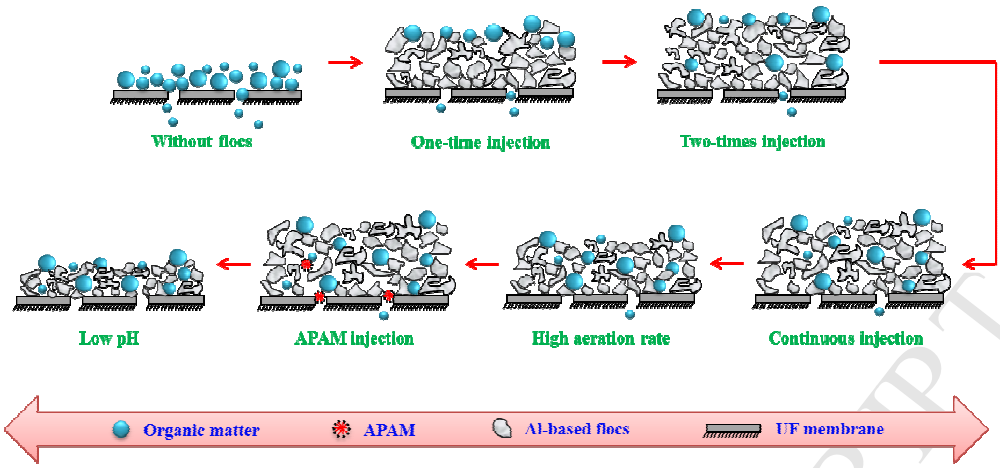

Fig. 8. Schematic diagram of the membrane fouling alleviation with multiple dynamic floc layers.

Highlights

- Al-based flocs were directly injected into UF membrane tank with bottom aeration.
- Membrane fouling was significantly alleviated by multiple dynamic floc layers.
- Solution pH played an important role on the properties of dynamic floc layers.
- Excellent performance was exhibited with the integrated filtration by raw water.